

Supporting information:

	Phase composition before CNT oxidation	Precursors for sol-gel reaction
1	$\gamma\text{-Al}_2\text{O}_3$	Aluminium nitrate
2	SiO_2	Tetraethyl orthosilicate
3	$\beta\text{-ZrO}_2$	Zirconium- <i>n</i> -propoxide
4	WO_3	Tungsten ethoxide
5	ZnO	Zinc nitrate
6	Fe_2O_3	Iron nitrate
7	SnO_2	Tin chloride
8	Cr_2O_3	Chromium (III) acetylacetone
9	MgO	Magnesium nitrate
10	A-TiO ₂	Tetrabutyl orthotitanate
11	MoO_3	Molybdenum acetate
12	CuO	Copper sulfate
13	R-TiO ₂	Tetrabutyl orthotitanate
14	V_2O_5	Vanadyl <i>i</i> -propoxide
15	NiO	Nickel acetate
16	La_2O_3	Lanthanum nitrate
17	Mn, Mn_2O_3	Manganese acetate
18	CeO_2	Cerium (III) 2-ethylhexanoate
19	Co_3O_4	Copper acetate
20	PbO	Lead (II) oxide
21	$\beta\text{-Bi}_2\text{O}_3$	Bismuth-2-hexylhexanoate

Table S1: List of synthesised CNT-metal oxide hybrids including precursors for sol-gel reaction and phase composition before and after CNT oxidation.

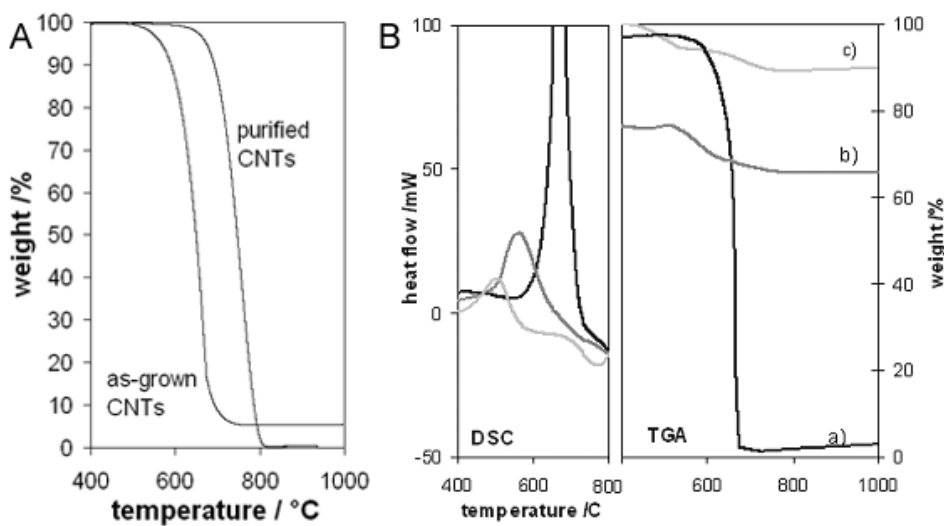


Figure S1: A) Weight loss curves for as-grown and purified CNTs showing a reduction in the residual weight from metal catalyst from 5 wt% to 0.5 wt% as well as an increased oxidation temperature due to the removal of amorphous carbon and metal residues. B) Combined weight loss and heat flow curves (TGA/DSC) for a) uncoated CNTs (as-grown) and CNTs coated with b) anatase-TiO₂ and c) rutile-TiO₂, modified from reference ⁸. The results show that the oxidation temperatures for the CNT-TiO₂ hybrids are reduced compared with the uncoated CNTs, in the order CNT-rutile < CNT-anatase < CNT.

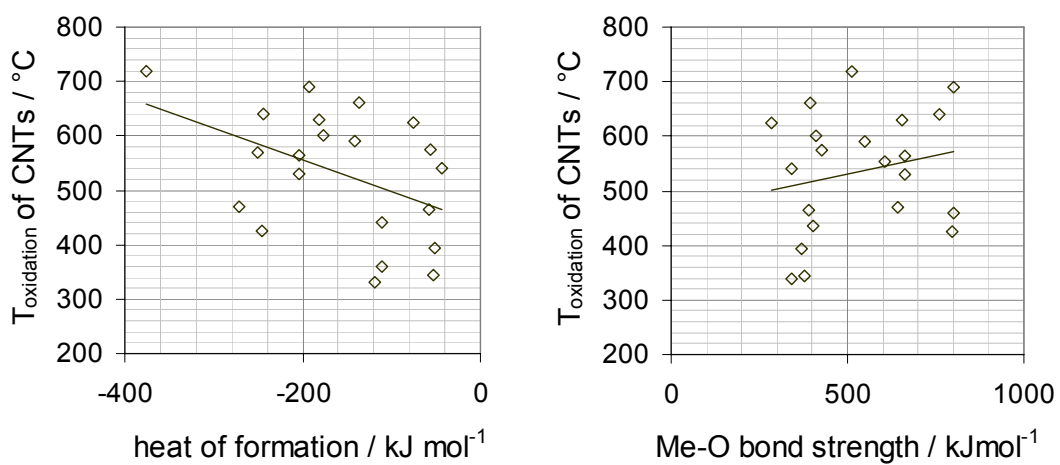


Figure S2: Relationships between the onset temperatures for CNT oxidation and literature data for (left) heat of formation of the metal oxides from lower oxides/metals and (right) metal-oxygen bond strength.

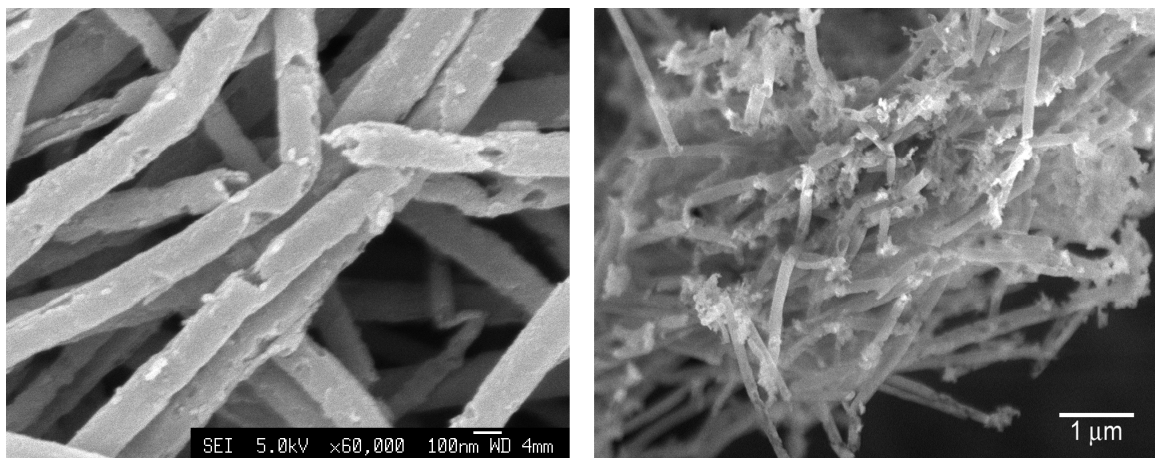


Figure S3: SEM images of CNT-WO₃ and CNT-ZrO₂ hybrids after a controlled careful oxidation of CNTs at temperatures a few degrees below T_{Ox}. The images show that the tubular structure of WO₃ and ZrO₂ is preserved.